Redox Biology 7 (2016) 14–20

Contents lists available at ScienceDirect

Redox Biology

journal homepage: www.elsevier.com/locate/redox

Research Paper

Cysteines 208 and 241 in Ero1α are required for maximal catalytic turnover

Thomas Ramming [a,1], Shingo Kanemura [b,1], Masaki Okumura [b], Kenji Inaba [b], Christian Appenzeller-Herzog [a,2]

[a] Division of Molecular & Systems Toxicology, Department of Pharmaceutical Sciences, University of Basel, 4056, Basel, Switzerland
[b] Institute of Multidisciplinary Research for Advanced Materials, Tohoku University Katahira 2-1-1, Sendai, 980-8577, Japan

ARTICLE INFO

Article history:
Received 10 October 2015
Received in revised form
11 November 2015
Accepted 12 November 2015
Available online 14 November 2015

Keywords:
Ero1α
PDI
Disulfide bond
Redox homeostasis
Endoplasmic reticulum

ABSTRACT

Endoplasmic reticulum (ER) oxidoreductin 1α (Ero1α) is a disulfide producer in the ER of mammalian cells. Besides four catalytic cysteines (Cys^{94}, Cys^{99}, Cys^{394}, Cys^{397}), Ero1α harbors four regulatory cysteines (Cys^{104}, Cys^{131}, Cys^{208}, Cys^{241}). These cysteines mediate the formation of inhibitory intramolecular disulfide bonds, which adapt the activation state of the enzyme to the redox environment in the ER through feedback signaling. Accordingly, disulfide production by Ero1α is accelerated by reducing conditions, which minimize the formation of inhibitory disulfides, or by mutations of regulatory cysteines. Here we report that reductive stimulation enhances Ero1α activity more potently than the mutation of cysteines. Specifically, mutation of Cys^{208}/Cys^{241} does not mechanistically mimic reductive stimulation, as it lowers the turnover rate of Ero1α in presence of a reducing agent. The Cys^{208}/Cys^{241} pair therefore fulfills a function during catalysis that reaches beyond negative regulation. In agreement, we identify a reciprocal crosstalk between the stabilities of the Cys^{208}–Cys^{241} disulfide and the inhibitory disulfide bonds involving Cys^{104} and Cys^{131}, which also controls the recruitment of the H_2O_2 scavenger GPx8 to Ero1α. Two possible mechanisms by which thiol–disulfide exchange at the Cys^{208}/Cys^{241} pair stimulates the catalytic turnover under reducing conditions are discussed.

1. Introduction

The synthesis of extracellular proteins is initiated at the endoplasmic reticulum (ER) where translating ribosomes translocate the nascent polypeptides into the ER lumen. Many of these polypeptides subsequently acquire critical covalent linkages between cysteine residues (termed disulfide bonds) through thiol-disulfide exchange reactions. Among the different systems for disulfide bond formation in the ER, ER oxidoreductin 1 (Ero1)-catalyzed oxidation of the active-site cysteine pair in protein disulfide isomerase (PDI) constitutes the best-conserved pathway [1,2]. Ero1 in vertebrates exists in two isoforms, Ero1α and Ero1β, whereas Ero1α is ubiquitously expressed and being viewed as the major source of disulfides in humans [3].

The flavoprotein Ero1α is an oxidase that couples the reduction of molecular oxygen (O_2) to disulfide-bond formation [3]. In the reductive phase of the Ero1α catalytic cycle, the flavin adenine dinucleotide (FAD) cofactor in Ero1α is reduced to $FADH_2$ as a result of disulfide transfer from Ero1α to reduced PDI (PDI_{red}). The reaction is catalyzed by an outer active-site cysteine pair (Cys^{94}/Cys^{99}), which shuttles two electrons from PDI_{red} *via* an inner active-site cysteine pair (Cys^{394}/Cys^{397}) to FAD. This process is tightly regulated by the reversible formation of two inhibitory disulfides (Cys^{94}–Cys^{131} and Cys^{99}–Cys^{104}) [4–6]. In the oxidative phase, FAD is regenerated by the transfer of two electrons onto O_2, which leads to the formation of one molecule of hydrogen peroxide (H_2O_2) [7]. Recent evidence indicates that H_2O_2 is instantaneously reduced to H_2O by the Ero1α-associated glutathione peroxidase family enzymes GPx7 or GPx8, which also introduce the resulting second disulfide into PDI [8,9]. We showed that access of O_2 to the buried FAD molecule is negatively regulated by the Cys^{208}–Cys^{241} disulfide [10].

The thiol-disulfide statuses of all inhibitory disulfide bonds in Ero1α are governed by canonical PDI or other PDI family members [10,11]. Accordingly, regulatory cysteines fine-tune the activation state of Ero1α in a redox environment-dependent manner by blocking either the reductive (Cys^{104}, Cys^{131}) or the oxidative (Cys^{208}, Cys^{241}) phase of the catalytic cycle through the formation of feedback-regulated inhibitory disulfides in response to oxidizing conditions. Conversely, a reducing ER environment promotes

E-mail addresses: kinaba@tagen.tohoku.ac.jp (K. Inaba), Christian.Appenzeller@sbl.ch (C. Appenzeller-Herzog).
[1] Equal contribution
[2] current address: Berufsfachschule Gesundheit Baselland, 4142 Münchenstein, Switzerland

http://dx.doi.org/10.1016/j.redox.2015.11.004
2213-2317/

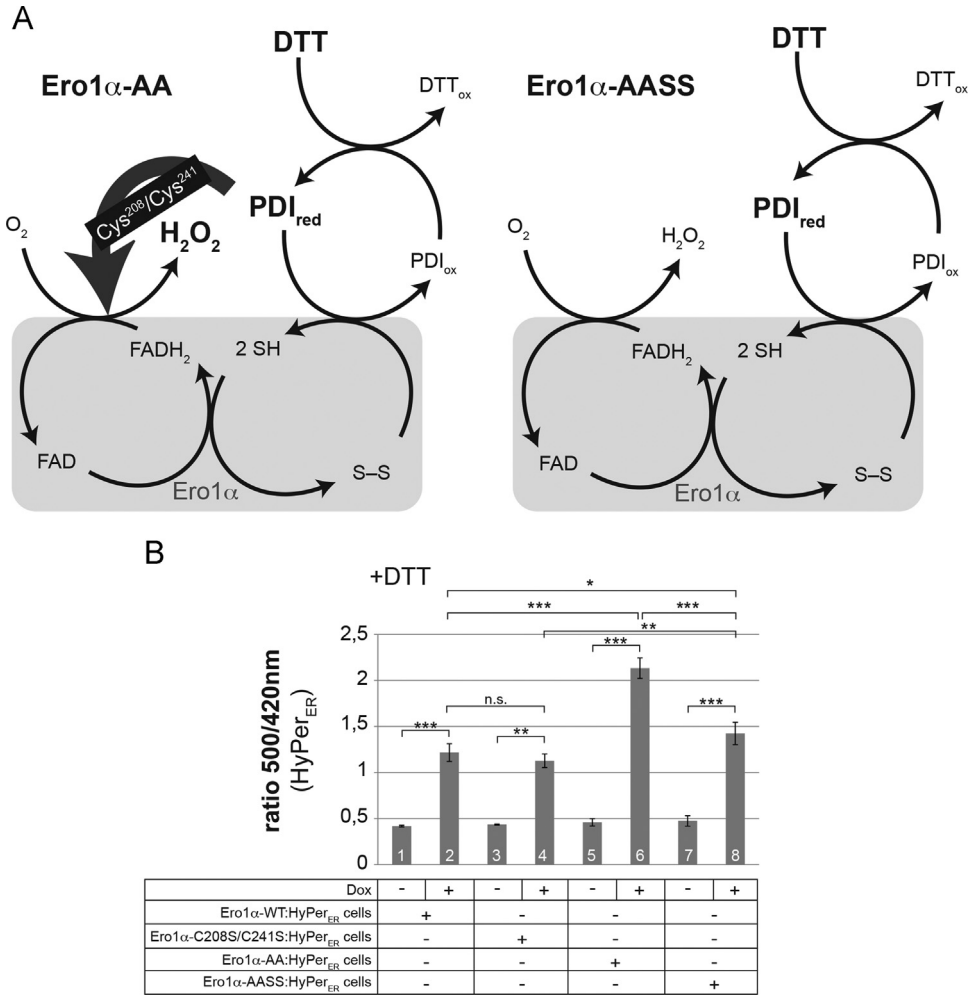

Fig. 1. (A) Schematic depicting the influence of DTT on the formation of Ero1α-derived H_2O_2 in the ER. The resulting high concentration of PDI_{red} exerts a stimulatory effect on Ero1α by catalyzing thiol-disulfide exchange at the regulatory disulfide between Cys^{208} and Cys^{241} (see main text for detailed models). (B) $HyPer_{ER}$ fluorescence excitation spectrum analyses of indicated cell lines measured 5 min after the addition of 0.5 mM DTT were performed. Plotted are the ratios of the 500 and 420 nm peak amplitudes ($n \geq 3$; mean ± SD). $^{*}p < 0.05$; $^{**}p < 0.01$; $^{***}p < 0.001$.

Ero1α activation through PDI-catalyzed reduction of these disulfides, as could for instance be important in response to physiological hypoxia or peak concentrations of reduced glutathione (GSH) or redox-active vitamins.

Here, we report that reducing conditions, which activate Ero1α through the removal of inhibitory disulfides, more potently stimulate Ero1α activity than the mutation of all regulatory cysteines. Thus, the presence of the Cys^{208}/Cys^{241} pair is required for maximal catalytic turnover under reducing conditions. Our data indicate a new mechanism of Ero1α regulation in which thiol-disulfide exchange at Cys^{208}–Cys^{241} affects the stability of the Cys^{94}–Cys^{131} inhibitory disulfide through allosteric and/or intermolecular communication.

2. Materials and methods

2.1. Fluorescence excitation spectrum analysis

Cells stably transfected with $HyPer_{ER}$ were subjected to fluorescence excitation spectrum analysis as described before [12].

2.2. Dithiothreitol (DTT) washout assays

The cellular glutathione disulfide:total glutathione ($GSSG:GS_{tot}$) ratio after DTT washout was measured using a 5,5'-dithiobis(2-nitrobenzoic acid)/glutathione reductase recycling assay as previously described [13].

2.3. Statistics

Data sets were analyzed for statistical significance using Student's *t* test (two-tailed distribution; heteroscedastic).

2.4. Cell culture and transient transfections

The culturing of HeLa cells [14] and FlipIn TRex293 cells for doxycycline (1 μg/ml, Sigma)-inducible expression of Ero1 variants [4] has been described. The following FlipIn TRex293 cell lines have been published previously: Ero1α [4], Ero1α-AA [6], Ero1α-C208S/C241S, Ero1α-AASS [10], Ero1α-AA:$HyPer_{ER}$ [8], Ero1α-C208S/C241S:$HyPer_{ER}$ [10] and Ero1α-AASS:$HyPer_{ER}$ [10]. The Ero1α−WT:$HyPer_{ER}$ cell line was created as before [8] (with the $HyPer_{ER}$ vector kindly provided by Miklos Geiszt, Semmelweis University, Hungary).

Transient transfections of HeLa cells were carried out using Turbofect (Thermo Scientific). Transient transfections of FlipIn TRex293 cells were carried out using Metafectene Pro (Biontex).

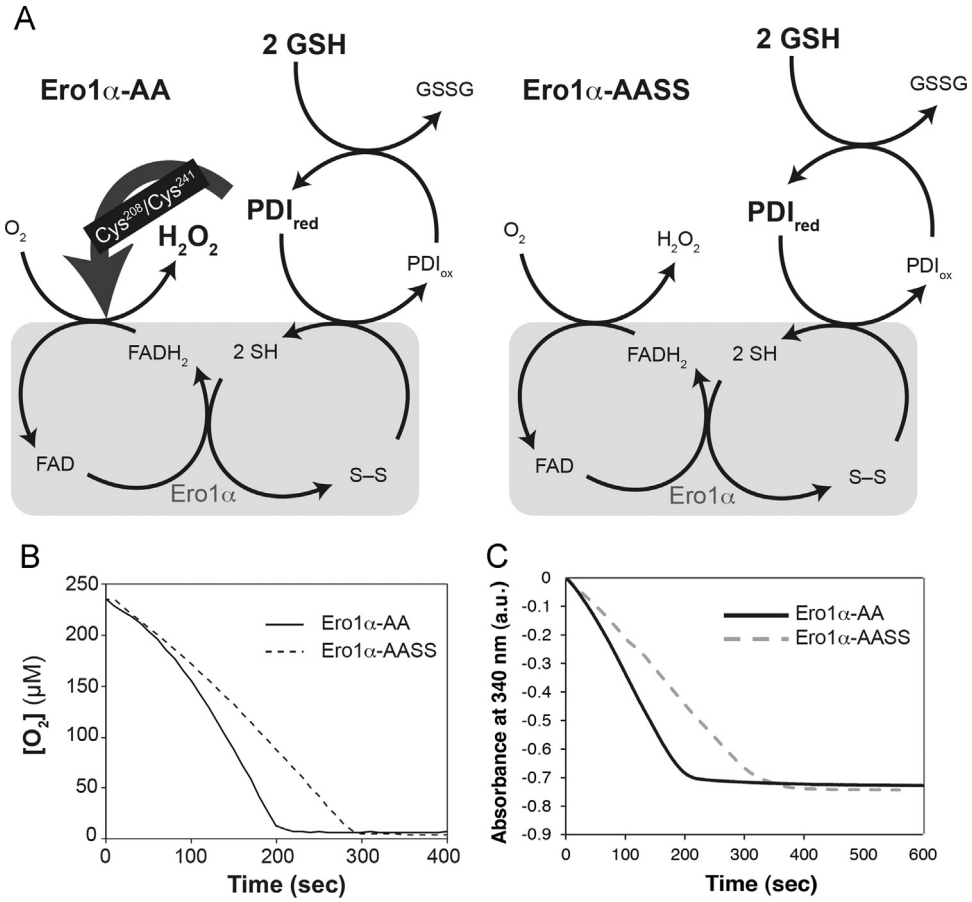

Fig. 2. (A) Schematic depicting the influence of GSH on the catalytic turnover of Ero1α *in vitro*. The resulting high concentration of PDI_{red} exerts a stimulatory effect on Ero1α by catalyzing thiol-disulfide exchange at the regulatory disulfide between Cys^{208} and Cys^{241} (see main text for detailed models). (B) O_2 consumption was monitored over time in a mixture of 2 μM Ero1α-AA (solid line) or Ero1α-AASS (dashed line), 10 μM PDI, and 10 mM GSH. (C) Consumption of NADPH coupled to catalysis by Ero1α-AA (solid line) or Ero1α-AASS (dashed line) (see Materials and Methods; 2 μM Ero1α variants, 10 μM PDI, 1 mM GSH, 1 U glutathione reductase, 200 μM NADPH) was detected by following the absorbance at 340 nm.

2.5. Oxygen and NADPH consumption assay

Oxygen consumption was measured as previously described [15]. Experimental procedure of NADPH consumption assay has been described before [16,17].

2.6. Determination of the redox equilibrium constant (Keq)

K_{eq} values of Cys^{94}–Cys^{131} in Ero1α-WT and Ero1α-C208S/C241S were determined as follows. Ero1α-WT or Ero1α-C208S/C241S (2 μM) was incubated for 30 min at 30 °C in degassed 50 mM Tris/HCl (pH 7.5) buffer containing 300 mM NaCl, 0.2 mM GSSG and various concentrations of GSH (0.2–4 mM). After incubation, 1 mM NEM was added to avoid subsequent redox reactions. All the samples were separated by non-reducing SDS-PAGE and stained with Coomassie brilliant blue (CBB). The values of fraction of OX2 state of Ero1α were estimated by LAS-3000 image reader, and plotted against $[GSH]^2/[GSSG]$ ratios. K_{eq} values were determined by fitting the data according to equation:

$$R = ([GSH]^2/[GSSG])/\{Keq + ([GSH]^2/[GSSG])\}$$

where R is fraction of OX2 state of Ero1α at equilibrium.

2.7. Bimolecular fluorescence complementation (BiFC) assay

HeLa cells were transfected and analyzed as previously described [10]. CRTss+EYFP1+mature Ero1α in pcDNA3.1 (dubbed EYFP1–Ero1α-WT) and CRTss+EYFP2+luminal domain GPx8 in pcDNA3.1 (dubbed EYFP2–$GPx8_{lum}$) were kindly provided by Lloyd Ruddock [18]. EYFP1–Ero1α-AA was generated by site-directed mutagenesis.

3. Results and discussion

Recent work has demonstrated that Ero1α-AASS, an Ero1α variant with all four regulatory cysteines being mutated (C104A, C131A, C208S, C241S), displays higher oxidase activity than Ero1α-AA where only Cys^{104} and Cys^{131} are mutated [10]. A likely mechanism was presented in which PDI_{red} facilitates the reaction of $FADH_2$ with O_2 in Ero1α-AA by opening the intramolecular Cys^{208}–Cys^{241} disulfide [10]. Since PDI_{red} is depleted through the oxidation by Ero1α-AA and its regeneration from oxidized PDI (PDI_{ox}) is relatively inefficient in the ER at steady state, the reaction rate is limited by the availability of PDI_{red}. Accordingly, Ero1α-AASS, which lacks Cys^{208}–Cys^{241}, generates higher amounts of the reaction products PDI_{ox} and H_2O_2, as it is active irrespectively of the scarcity of PDI_{red} [10].

In cells, oxidase activity of wild-type Ero1α (Ero1α-WT) or Ero1α-AA can be stimulated by the addition of the membrane-permeable reductant dithiothreitol (DTT). This manifests in a more prominent detection of the reaction product H_2O_2 in the ER of Ero1α-overexpressing cells [8,10,19,20] and can mechanistically be explained by DTT-stimulated reduction of inhibitory disulfides in Ero1α [4–6,10,21]. In case of Ero1α-AA, DTT-mediated activation is connected to the enhanced opening of Cys^{208}–Cys^{241} by PDI_{red}

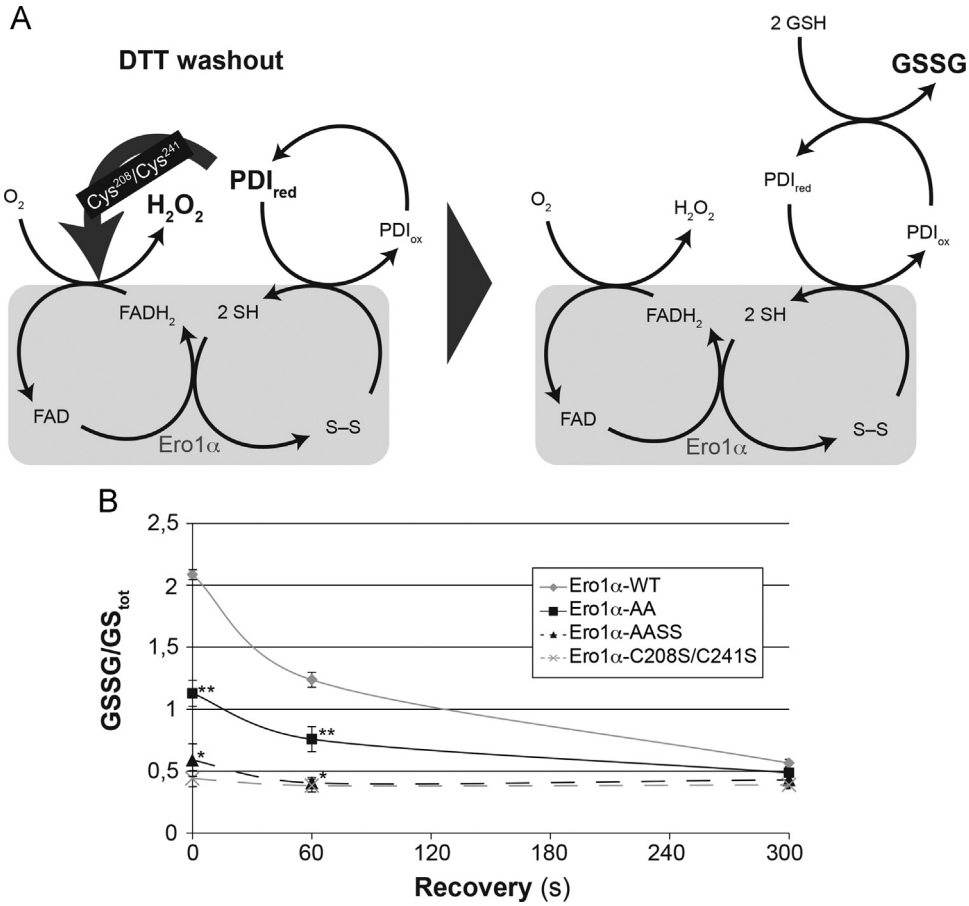

Fig. 3. (A) Schematic depicting the reactions leading to GSSG formation following DTT washout in Ero1α-overexpressing cells. (B) $GSSG/GS_{tot}$ recovery curves upon DTT washout were compared between Ero1α-WT-, Ero1α-AA-, Ero1α-AASS- and Ero1α-C208S/C241S-expressing cells. (mean ± SEM; two independent experiments each performed at least in doublet). Statistically significant differences in the 0 and 60 s time point are indicated in the case of Ero1α-AA (compared to Ero1α-WT; $^{**}p < 0.01$) and in the case of Ero1α-AASS (compared to Ero1α-AA; $^{*}p < 0.05$).

(Fig. 1A, left panel) [10].

Based on the data summarized above, Ero1α-AASS might be hyperactive, because it mimics the DTT-activated state of Ero1α-AA. To test this possibility, we examined to what extent DTT influences Ero1α-AASS-catalyzed production of H_2O_2. We used a cell line that expresses Ero1α-AASS only in presence of doxycycline and stably harbors the H_2O_2-sensitive fluorescent protein HyPer in the ER ($HyPer_{ER}$) [10,22]. $HyPer_{ER}$, the fluorescence excitation spectrum of which does not overlap with the one of doxycycline [12], is prone to oxidation not only by H_2O_2 but also by PDI_{ox} [23,24]. In DTT-treated cells, however, the oxidation of $HyPer_{ER}$ can basically be ascribed to H_2O_2 only, as DTT raises the concentration of Ero1α-derived H_2O_2 but lowers the levels of PDI_{ox} [21] (Fig. 1A, left panel). Using this model system in presence of 0.5 mM DTT, we analyzed the fold-increase in $HyPer_{ER}$ oxidation in cells treated with doxycycline as compared to untreated cells. We found that expression of Ero1α-AASS did not lead to equal or stronger production of H_2O_2 compared to Ero1α-AA. Rather, doxycycline-induced $HyPer_{ER}$ oxidation was lowered by ~40% in Ero1α-AASS expressing cells (Fig. 1B, bars 6 and 8). Likewise, expression of Ero1α-C208S/C241S trended to induce less prominent $HyPer_{ER}$ oxidation than that of Ero1α-WT (Fig. 1B, bars 2 and 4), whereas mutation of Cys^{104} and Cys^{131} increased oxidase activity as expected (Fig. 1B, bars 2 and 6, bars 4 and 8).

These findings were incompatible with the notion that Ero1α-AASS mimics the DTT-activated state of Ero1α-AA. Apparently, the Cys^{208}/Cys^{241} pair is required for full catalytic activity of Ero1α under reducing conditions. Since mutation of these cysteines precludes the thiol-disulfide exchange reactions that engage PDI to the O_2-reducing end of Ero1α, the stimulatory effect of PDI_{red} (Fig. 1A, left panel) drops out in these mutants. Thus, although poorly defined yet, the mechanism of PDI_{red}–mediated stimulation of Ero1α-AA cannot solely rely on the removal of the Cys^{208}–Cys^{241} disulfide.

We next examined if these new findings could also be recapitulated in a reconstituted system. Previously, we compared the performance of Ero1α-AA and Ero1α-AASS in oxidizing a one-time bolus of their substrate PDI_{red} [10]. In this setting, PDI_{ox} was generated faster in the Ero1α-AASS- compared with the Ero1α-AA-catalyzed reaction. Furthermore, purified Ero1α-AASS produced significantly higher levels of H_2O_2 compared to Ero1α-AA [10]. In order to mimic the situation in the ER of DTT-treated cells where PDI_{red} is constantly being regenerated, we added an excess of GSH to the reaction (Fig. 2A). This setup matches the commonly used practice to assay the oxidase activity of Ero1α *in vitro* [5,7,15–17,25]. Consistent with the results presented in Fig. 1B, the O_2 concentration dropped less rapidly in presence of Ero1α-AASS compared to Ero1α-AA when GSH was added to the reaction (Fig. 2B). Similarly, in an assay that indirectly detects the formation of GSSG by monitoring glutathione reductase-dependent consumption of NADPH [16], Ero1α-AASS displayed lower oxidase activity than Ero1α-AA (Fig. 2C). Altogether, these experiments confirmed that Ero1α-AASS is catalytically hampered relative to Ero1α-AA under reductively stimulated conditions, which contrasts with the situation in the absence of excess reducing agent [10].

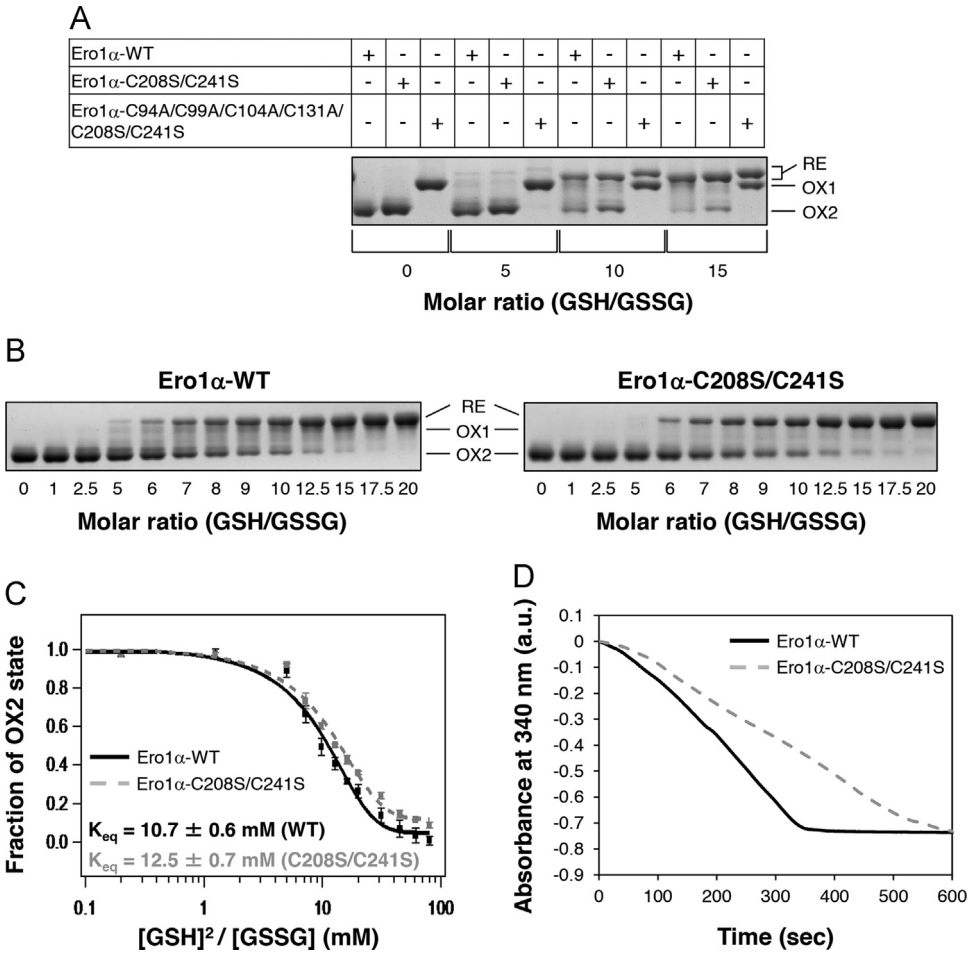

Fig. 4. (A) Redox equilibrium of Ero1α-WT, Ero1α-C208S/C241S and Ero1α-C94A/C99A/C104A/C131A/C208S/C241S in presence of GSH/GSSG. All the samples were incubated for 30 min with different GSH/GSSG ratios under anaerobic condition at 30 °C and modified by NEM. The redox states of the Ero1α derivatives were separated by non-reducing SDS-PAGE and stained with CBB. "OX2" indicates the Ero1α species with the Cys^{94}–Cys^{131} regulatory disulfide. In "OX1", this disulfide is reduced or absent. "RE" indicates an Ero1α species in which not only Cys^{94}–Cys^{131} but also unidentified additional disulfide(s) are reduced. Note that the mobility of the "RE" species of Ero1α-WT or Ero1α-C208S/C241S is not exactly identical to that of Ero1α-C94A/C99A/C104A/C131A/C208S/C241S on a SDS gel, probably due to the presence of Cys^{99}-Cys^{104} disulfide in the former two. (B) Redox states of Ero1α-WT and Ero1α-C208S/C241S in wider ranges of GSH/GSSG ratio were analyzed as in (A). (C) Fraction of Ero1α in OX2 form is plotted against $[GSH]^2/[GSSG]$ ratios. K_{eq} values were determined from at least two independent experiments as follows: 10.7 ± 0.6 for Ero1α-WT (solid line) and 12.5 ± 0.7 for Ero1α-C208S/C241S (dashed line) (mean ± SD). (D) Consumption of NADPH coupled to catalysis of PDI oxidation by Ero1α-WT (solid line) or Ero1α-C208S/C241S (dashed line) (see Materials and Methods; 2 μM Ero1α variants, 10 μM PDI, 1 mM GSH, 1 U glutathione reductase, 200 μM NADPH).

Oxidase activity of Ero1α in the ER of live cells can also be assessed using a DTT washout approach that is coupled to the time-resolved quantification of the cellular $GSSG:GS_{tot}$ [8,10,13]. Because Ero1α is activated by DTT (Fig. 1A), the levels of PDI_{red} drop and GSSG builds up rapidly in response to DTT removal through the Ero1α–PDI–GSH cascade (Fig. 3A). Furthermore, the peroxidase-catalyzed reduction of H_2O_2 contributes to the build-up of GSSG [8] (not depicted in the figure). Ectopic over-expression of Ero1α is evidently reflected in the time-course of $GSSG:GS_{tot}$ after DTT washout. Thus, in cells that over-express Ero1α-WT, $GSSG:GS_{tot}$ transiently rises to about 500% of its steady-state value in the time-scale of seconds [13,26]. This massive accumulation of GSSG is followed by a decline and the restoration of the steady-state $GSSG:GS_{tot}$ in the time scale of minutes, which depends on cytosolic glutathione reductase [8] and the reformation of the inhibitory Cys^{208}–Cys^{241} disulfide in Ero1α [10].

Consistent with the results in Fig. 1B where over-expressed C208S/C241S mutants displayed lower oxidase activity than their unmutated counterparts in presence of DTT, mutation of the Cys^{208}/Cys^{241} pair decreased the Ero1α-dependent accumulation of GSSG upon DTT washout (Fig. 3B, compare the solid and the dashed lines). Unexpectedly, however, over-expression of Ero1α-AA led to a smaller peak in $GSSG:GS_{tot}$ upon DTT washout compared to over-expression of Ero1α-WT (Fig. 3B), although Ero1α-AA is catalytically more active than Ero1α-WT under reductively stimulated conditions (Figs. 1B, 2C and 4D). This may suggest that the decline of $GSSG:GS_{tot}$ in Ero1α-AA-expressing cells has already proceeded to significant extent before the assay period. It might also be possible that the constitutive absence of the regulatory Cys^{94}–Cys^{131} and Cys^{99}–Cys^{104} disulfides in the C104A/C131A mutant affects the Ero1α activity by altering the stability of the Cys^{208}–Cys^{241} disulfide in an allosteric and/or intermolecular manner (see the following paragraphs for more details).

To address the potential crosstalk between the Cys^{208}/Cys^{241} pair and the Cys^{94}–Cys^{131} regulatory disulfide bond, we measured the reduction potential of Cys^{94}–Cys^{131} in Ero1α-WT and Ero1α-C208S/C241S. As shown in Fig. 4A, purified Ero1α-WT was predominantly in an inactive form (OX2), which harbors the Cys^{94}–Cys^{131} disulfide [4] and migrates faster on a non-reducing SDS gel than the active OX1 form comprising the active-site Cys^{94}–Cys^{99} disulfide. Incubation of Ero1α-WT and Ero1α-C208S/C241S in various GSH/GSSG ratios followed by non-reducing SDS-PAGE revealed that indeed, the Cys^{208}/Cys^{241} pair influences the stability of the Cys^{94}–Cys^{131} disulfide. The C208S/C241S mutations slightly but significantly stabilized the Cys^{94}–Cys^{131} disulfide; the redox

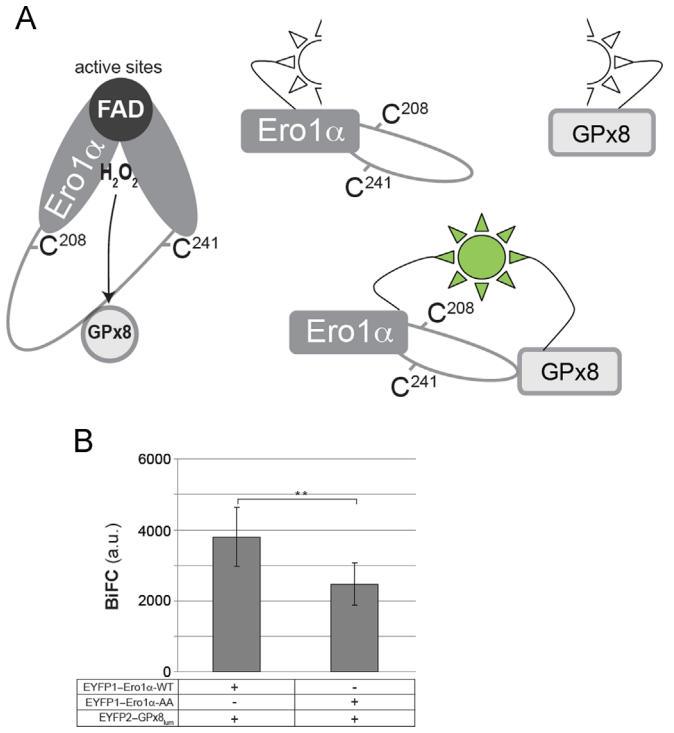

Fig. 5. (A) Schematic representation of the interaction of the luminal domain of GPx8 with the loop region between Cys^{208} and Cys^{241} in Ero1α (left panel) and the Bi-molecular fluorescence complementation (BiFC) of two YFP half-sites fused to either Ero1α or GPx8 (right panel). (B) 18 h after transfection with the indicated constructs, HeLa cells were trypsinized and analyzed by flow cytometry for BiFC fluorescence ($n \geq 5$; mean ± SD). a.u. arbitrary unit, $^{**}p < 0.01$.

equilibrium constant (K_{eq}) of Cys^{94}–Cys^{131} in Ero1α-WT is 10.7 ± 0.6 mM and that in Ero1α-C208S/C241S is 12.5 ± 0.7 mM (Figs. 4B and C). It is thus conceivable that the cleavage or absence of Cys^{208}–Cys^{241} leads to a higher propensity for the inactive OX2 form. In agreement, Ero1α-C208S/C241S was less active in oxidizing PDI than Ero1α-WT (Fig. 4D).

We next analyzed the binding of the GPx8 peroxidase to the Cys^{208}/Cys^{241} region in Ero1α [10]. In the bimolecular fluorescence complementation assay, the fluorescence of two combined yellow fluorescent protein half sites, which are fused with Ero1α and the ER-luminal domain of GPx8, respectively, is quantified [18] (Fig. 5A). Similar to the formation of Cys^{208}–Cys^{241}, docking of GPx8 is a process that takes place on the distal side of Ero1α relative to the active sites and the cofactor-binding site (Fig. 5A). The binding intensity of GPx8 was influenced by the presence or absence of the regulatory Cys^{94}–Cys^{131} and Cys^{99}–Cys^{104} disulfides: EYFP1–Ero1α-WT recruited ~50% more EYFP2–$GPx8_{lum}$ than EYFP1–Ero1α-AA (Fig. 5B). According to our previously proposed model, the recruitment of GPx8 occurs in response to the opening of Cys^{208}–Cys^{241} by PDI_{red} [10]. The data therefore underscored the notion that formation of the regulatory Cys^{94}–Cys^{131} disulfide in Ero1α-WT destabilized the Cys^{208}–Cys^{241} disulfide, thereby facilitating the recruitment of GPx8.

Altogether, two possible mechanisms underlying our finding that the Cys^{208}/Cys^{241} pair is required for maximal catalytic turnover in Ero1α are proposed. In a first model, stimulation of the Ero1α catalytic turnover can be mediated by the destabilization of Cys^{94}–Cys^{131} and possibly Cys^{99}–Cys^{104} in response to the formation of Cys^{208}–Cys^{241}. The present data strongly suggest that the stabilities of the Cys^{208}–Cys^{241} disulfide and the inhibitory disulfide bonds involving Cys^{104} and Cys^{131} influence each other in reciprocal manner. The resulting thiol-disulfide oscillations at Cys^{208}/Cys^{241} that are a predicted consequence of this model could be catalyzed by PDI or by other PDI family members such as ERp57 [10]. In this connection, a minor fraction of purified Ero1α can transiently be detected with fully reduced Cys^{208}/Cys^{241} pair upon addition of PDI_{red}, demonstrating that at least *in vitro* the dithiol form of Cys^{208}/Cys^{241} is generated during the Ero1α catalysis of PDI oxidation (Kanemura, S. and Inaba, K., manuscript in preparation).

In a second model, the specific architecture of the covalent Cys^{208}/Cys^{241}-linked Ero1α–PDI complex (previously termed Ero1α–PDI^{fast} [10]) is important, e.g. for the optimal channeling of O_2 to the active site. This possibility would be in agreement with a previous working model of the Ero1α catalytic cycle, which accommodated the remarkably high levels of Ero1α–PDI^{fast} in the ER [10]. According to this working model, Cys^{208}/Cys^{241} can hardly be found in the ER in the reduced dithiol state that resembles Ero1α-AASS, as Ero1α–PDI^{fast} is kinetically stabilized. In the same vein, the fact that Ero1α-AA but not Ero1α-AASS associates with the natural binding partner GPx8 through its Cys^{208}/Cys^{241} region (likely in the context of Ero1α–PDI^{fast}) underscores the non-native behavior of Ero1α-AASS [10].

It is important to note that these two mechanistic explanations are not exclusive to each other. Thus, a slightly modified, "mixed" model is possible where it is the formation of the Ero1α–PDI^{fast} complex that stabilizes the inhibitory disulfide bonds involving Cys^{104} and Cys^{131}. Conversely, reduction of Cys^{94}–Cys^{131} and Cys^{99}–Cys^{104} could promote the reformation of Cys^{208}–Cys^{241} from Ero1α–PDI^{fast}. It will be interesting to more closely characterize the communication between the opposing Cys^{94}/Cys^{131}/Cys^{99}/Cys^{104} end and the Cys^{208}/Cys^{241} end of Ero1α. It could be based on allostery or, alternatively, intermolecular catalysis either directly between two Ero1α molecules or indirectly *via* the redox state of PDI or GSH.

In this work, we present the new finding that Ero1α-AASS, which likely adopts a conformation equivalent to fully reduced Ero1α (disregarding catalytic and structural disulfides), does not reach the maximal catalytic turnover rate. Rather, the highest intrinsic activity is reached in presence of the Cys^{208}/Cys^{241} pair and a reducing agent, which ensures unlimited supply of PDI_{red}. We conclude that Cys^{208}/Cys^{241} plays an unexpected stimulatory role during catalysis. Cys^{208}/Cys^{241}-dependent stimulation could be due to optimized O_2 penetration into the Ero1α–PDI^{fast} complex and/or the destabilization of Cys^{94}–Cys^{131} and Cys^{99}–Cys^{104} in response to the oxidation of the Cys^{208}/Cys^{241} pair. Future experiments designed to elucidate these mechanistic possibilities will further increase our understanding of regulated disulfide-bond formation in the ER.

Acknowledgment

This work was supported by a PhD fellowship by the Boehringer Ingelheim Fonds (to TR), the Swiss National Science Foundation (Ambizione), the University of Basel, and the Freiwillige Akademische Gesellschaft (all to CAH), CREST, JST (to K. I.), Grant-in-Aids for Scientific Research on Innovative Areas from MEXT (to K. I. and M. O.), Takeda Science Foundation (to K. I.) and Grant-in-Aids for JSPS Fellows (to S. K. and M. O.).

References

[1] K. Araki, K. Inaba, Structure, mechanism, and evolution of Ero1 family enzymes, Antioxid. Redox Signal. 16 (2012) 790–799.
[2] O.B. Oka, N.J. Bulleid, Forming disulfides in the endoplasmic reticulum, Biochim. Et. Biophys. Acta 1833 (2013) 2425–2429.
[3] T. Ramming, C. Appenzeller-Herzog, The physiological functions of mammalian endoplasmic oxidoreductin 1: on disulfides and more, Antioxid. Redox

Signal. 16 (2012) 1109–1118.
[4] C. Appenzeller-Herzog, J. Riemer, B. Christensen, E.S. Sorensen, L. Ellgaard, A novel disulphide switch mechanism in Ero1alpha balances ER oxidation in human cells, EMBO J. 27 (2008) 2977–2987.
[5] K.M. Baker, S. Chakravarthi, K.P. Langton, A.M. Sheppard, H. Lu, N.J. Bulleid, Low reduction potential of Ero1alpha regulatory disulphides ensures tight control of substrate oxidation, EMBO J. 27 (2008) 2988–2997.
[6] H.G. Hansen, J.D. Schmidt, C.L. Soltoft, T. Ramming, H.M. Geertz-Hansen, B. Christensen, E.S. Sorensen, A.S. Juncker, C. Appenzeller-Herzog, L. Ellgaard, Hyperactivity of the Ero1alpha oxidase elicits endoplasmic reticulum stress but no broad antioxidant response, J. Biol. Chem. 287 (2012) 39513–39523.
[7] L. Wang, S.J. Li, A. Sidhu, L. Zhu, Y. Liang, R.B. Freedman, C.C. Wang, Reconstitution of human Ero1-Lalpha/protein-disulfide isomerase oxidative folding pathway in vitro. Position-dependent differences in role between the a and a' domains of protein-disulfide isomerase, J. Biol. Chem. 284 (2009) 199–206.
[8] T. Ramming, H.G. Hansen, K. Nagata, L. Ellgaard, C. Appenzeller-Herzog, GPx8 peroxidase prevents leakage of H2O2 from the endoplasmic reticulum, Free Radic. Biol. Med. 70 (2014) 106–116.
[9] L. Wang, L. Zhang, Y. Niu, R. Sitia, C.C. Wang, Glutathione peroxidase 7 utilizes hydrogen peroxide generated by Ero1alpha to promote oxidative protein folding, Antioxid. redox Signal. 20 (2014) 545–556.
[10] T. Ramming, M. Okumura, S. Kanemura, S. Baday, J. Birk, S. Moes, M. Spiess, P. Jeno, S. Berneche, K. Inaba, C. Appenzeller-Herzog, A PDI-catalyzed thiol-disulfide switch regulates the production of hydrogen peroxide by human Ero1, Free. Radic. Biol. Med. 83 (2015) 361–372.
[11] C. Shepherd, O.B. Oka, N.J. Bulleid, Inactivation of mammalian Ero1alpha is catalysed by specific protein disulfide-isomerases, Biochem. J. 461 (2014) 107–113.
[12] J. Birk, T. Ramming, A. Odermatt, C. Appenzeller-Herzog, Green fluorescent protein-based monitoring of endoplasmic reticulum redox poise, Front. Genet. 4 (2013) 108.
[13] C. Appenzeller-Herzog, J. Riemer, E. Zito, K.T. Chin, D. Ron, M. Spiess, L. Ellgaard, Disulphide production by Ero1alpha-PDI relay is rapid and effectively regulated, EMBO J. 29 (2010) 3318–3329.
[14] J. Birk, M. Meyer, I. Aller, H.G. Hansen, A. Odermatt, T.P. Dick, A.J. Meyer, C. Appenzeller-Herzog, Endoplasmic reticulum: reduced and oxidized glutathione revisited, J. Cell. Sci. 126 (2013) 1604–1617.
[15] K. Inaba, S. Masui, H. Iida, S. Vavassori, R. Sitia, M. Suzuki, Crystal structures of human Ero1alpha reveal the mechanisms of regulated and targeted oxidation of PDI, EMBO J. 29 (2010) 3330–3343.
[16] Y. Sato, R. Kojima, M. Okumura, M. Hagiwara, S. Masui, K. Maegawa, M. Saiki, T. Horibe, M. Suzuki, K. Inaba, Synergistic cooperation of PDI family members in peroxiredoxin 4-driven oxidative protein folding, Sci. Rep. 3 (2013) 2456.
[17] M. Okumura, H. Kadokura, S. Hashimoto, K. Yutani, S. Kanemura, T. Hikima, Y. Hidaka, L. Ito, K. Shiba, S. Masui, D. Imai, S. Imaoka, H. Yamaguchi, K. Inaba, Inhibition of the functional interplay between endoplasmic reticulum (ER) oxidoreductin-1alpha (Ero1alpha) and protein-disulfide isomerase (PDI) by the endocrine disruptor bisphenol A, J. Biol. Chem. 289 (2014) 27004–27018.
[18] V.D. Nguyen, M.J. Saaranen, A.R. Karala, A.K. Lappi, L. Wang, I.B. Raykhel, H. I. Alanen, K.E. Salo, C.C. Wang, L.W. Ruddock, Two endoplasmic reticulum PDI peroxidases increase the efficiency of the use of peroxide during disulfide bond formation, J. Mol. Biol. 406 (2011) 503–515.
[19] Z. Cao, S. Subramaniam, N.J. Bulleid, Lack of an efficient endoplasmic reticulum-localized recycling system protects peroxiredoxin IV from hyperoxidation, J. Biol. Chem. 289 (2014) 5490–5498.
[20] T.J. Tavender, N.J. Bulleid, Peroxiredoxin IV protects cells from oxidative stress by removing H2O2 produced during disulphide formation, J. Cell. Sci. 123 (2010) 2672–2679.
[21] A. Delaunay-Moisan, C. Appenzeller-Herzog, The antioxidant machinery of the endoplasmic reticulum: Protection and signaling, Free. Radic. Biol. Med. 83 (2015) 341–351.
[22] B. Enyedi, P. Varnai, M. Geiszt, Redox state of the endoplasmic reticulum is controlled by Ero1L-alpha and intraluminal calcium, Antioxid. Redox Signal. 13 (2010) 721–729.
[23] I. Mehmeti, S. Lortz, S. Lenzen, The H2O2-sensitive HyPer protein targeted to the endoplasmic reticulum as a mirror of the oxidizing thiol-disulfide milieu, Free Radic. Biol. Med. 53 (2012) 1451–1458.
[24] L.W. Ruddock, Low-molecular-weight oxidants involved in disulfide bond formation, Antioxid. redox Signal. 16 (2012) 1129–1138.
[25] K. Araki, K. Nagata, Functional in vitro analysis of the ERO1 protein and protein-disulfide isomerase pathway, J. Biol. Chem. 286 (2011) 32705–32712.
[26] C. Appenzeller-Herzog, Glutathione- and non-glutathione-based oxidant control in the endoplasmic reticulum, J. Cell. Sci. 124 (2011) 847–855.